

1                   **DNA repair is essential for *Vibrio cholerae* growth on**  
2                   **Thiosulfate-Citrate-Bile Salts-Sucrose (TCBS) Medium**

3  
4   **Alex J. Wessel, Drew T.T. Johnson, and Christopher M. Waters\***

5   Department of Microbiology, Genetics, and Immunology, Michigan State University, East  
6   Lansing, Michigan, USA

7  
8   \* **Corresponding Author:**

9   5180 Biomedical and Physical Sciences

10   567 Wilson Road

11   East Lansing, MI 48824

12   Telephone 517-884-5360

13  
14   Short title: DNA repair is required for *V. cholerae* TCBS growth

15   Key Words: *Vibrio cholerae*, TCBS, Exo VII, DNA repair

16   Declarations of interest: none

17

18

19

20

21

22

23

24

## 25 **Abstract**

26 Thiosulfate-citrate-bile salts-sucrose (TCBS) agar is a selective and differential media  
27 for the enrichment of pathogenic *Vibrios*. We observed that an exonuclease VII (*exoVII*)  
28 mutant of *Vibrio cholerae* failed to grow on TCBS agar, suggesting that DNA repair  
29 mutant strains may be hampered for growth in this selective media. Examination of the  
30 selective components of TCBS revealed that bile acids were primarily responsible for  
31 toxicity of the *exoVII* mutant. Suppressor mutations in DNA gyrase restored growth of  
32 the *exoVII* mutants on TCBS, suggesting that TCBS inhibits DNA gyrase similar to the  
33 antibiotic ciprofloxacin. To better understand what factors are important for *V. cholerae*  
34 to grow on TCBS, we generated a randomly-barcoded TnSeq (RB-TnSeq) library in *V.*  
35 *cholerae* and have used it to uncover a range of DNA repair mutants that also fail to  
36 grow on TCBS agar. The results of this study suggest that TCBS agar causes DNA  
37 damage to *V. cholerae* similarly to the mechanism of action of fluoroquinolones, and  
38 overcoming this DNA damage is critical for *Vibrio* growth on this selective medium.

39

## 40 **Abstract Importance**

41 TCBS is often used to diagnose cholera infection. We found that many mutant *V.*  
42 *cholerae* strains are attenuated for growth on TCBS agar, meaning they could remain  
43 undetected using this culture-dependent method. Hypermutator strains with defects in  
44 DNA repair pathways might be especially inhibited by TCBS. In addition, *V. cholerae*  
45 grown successively on TCBS agar develops resistance to ciprofloxacin.

## 46 **Introduction**

47 *Vibrio cholerae* is the causative agent of cholera, a gastrointestinal infection  
48 characterized by profuse watery diarrhea that, when left untreated, causes rapid  
49 dehydration and death. This gram-negative bacterium lives a dual lifestyle, alternating  
50 between its aquatic environmental niche and human host environment where it is  
51 acquired through ingestion of contaminated food or water. Cholera remains endemic in  
52 much of the developing world, with sporadic outbreaks occurring in nations with poor  
53 sanitation practices and limited access to clean drinking water (1, 2).

54  
55 Culture confirmation from stool samples remains the gold standard for the diagnosis of  
56 *V. cholerae* infections (3). This is typically achieved using Thiosulfate-Citrate-Bile Salts-  
57 Sucrose (TCBS) agar, a highly selective medium for *Vibrios*. Following growth, the  
58 identity of a *Vibrio* grown on TCBS agar can be further determined based on its capacity  
59 to ferment sucrose— while *V. cholerae* can ferment sucrose, most other medically  
60 relevant *Vibrios* cannot (4).

61  
62 Aside from sucrose, the major selective factors in TCBS are the medium's alkaline pH  
63 and bile salts, which inhibit the growth of non-*Vibrio* enterics. Given that *V. cholerae*  
64 encounters bile routinely throughout its pathogenic lifecycle, it has evolved a variety of  
65 mechanisms to sense, respond to, and limit the antimicrobial effects of bile. To this end,  
66 bile represents a significant environmental signal in the pathogenesis of *V. cholerae*. *V.*  
67 *cholerae* senses bile through an interaction between the inner membrane sensory and  
68 regulatory proteins ToxR and ToxS (5, 6). For example, in the human intestinal tract, bile  
69 activation of ToxRS adapts *V. cholerae* for bile tolerance by inducing and inhibiting the

70 expression of outer membrane proteins OmpU and OmpT, respectively (7–9). Because  
71 bile can enter the cell through OmpT but not OmpU (10, 11), a shift in porin expression  
72 protects *V. cholerae* from its cytotoxic effects.

73

74 The bacterial stress response to bile is mostly characterized by DNA damage leading to  
75 SOS induction as well as the remodeling of the cell membrane (12–17). Early works in  
76 *E. coli* demonstrate that cell death and SOS induction in response to bile mimic that of  
77 cells treated with the DNA crosslinking agent mitomycin C, suggesting that bile may  
78 cause direct DNA damage in bacteria (18). Another study by Prieto and colleagues  
79 indicate that treatment of *Salmonella enterica* with bile causes oxidative DNA damage  
80 and increases the frequency of GC → AT transitions. This led the authors to suggest  
81 that base excision repair and recombinational repair, but not nucleotide excision repair,  
82 are necessary for *S. enterica* tolerance to bile (13).

83

84 In this work we demonstrate that exonuclease VII (*exoVII*) mutant *V. cholerae* fails to  
85 grow on TCBS agar, and that the main component in TCBS agar that is responsible for  
86 this inhibition is ox bile. We found that mutations in DNA gyrase (encoded by genes  
87 *gyrA* and *gyrB*) suppress the toxicity of TCBS in the absence of ExoVII and that some of  
88 these mutations confer resistance to the fluoroquinolone ciprofloxacin. Finally, we  
89 performed randomly barcoded transposon insertion site sequencing (RB-TnSeq) to  
90 identify other *V. cholerae* mutants with growth defects on TCBS agar, and in doing so  
91 uncovered mutants with component-dependent growth defects. The results presented  
92 here (19) provide an explanation for the inhibition of *exoVII* mutant *V. cholerae* and

93 suggest that bile salts/acids may induce quinolone-like DNA damage in bacteria.  
94 Moreover, we show that DNA repair is essential for *V. cholerae* to robustly grow on  
95 TCBS which has significant implications on whether TCBS can accurately sample the  
96 diversity of *V. cholerae* in clinical isolates.

97

## 98 **Results**

### 99 ***xseA* mutant *V. cholerae* cannot grow on TCBS agar.**

100 While conducting previously-described experiments to enhance the efficiency of  
101 Multiplex Genome Editing by Natural co-Transformation (MuGENT)(28), we  
102 serendipitously discovered that a *V. cholerae* mutant strain derived from the El Tor  
103 Biotype E7946 (strain TND0252: Ptac-*tfoX*,  $\Delta recJ$ 501bp,  $\Delta exoVII$ 501bp,  $\Delta lacZ::lacIq$ ,  
104  $\Delta vc1807::SpecR$ ), which had been developed to allow MuGENT with minimal homology  
105 regions, failed to grow on Thiosulfate-Citrate-Bile Salts-Sucrose (TCBS) agar, a  
106 selective and differential medium for *Vibrios*. However, the parental E7946 strain and  
107 another El Tor isolate that is widely used, C6706, grew well (Fig 1A). TND0252 has  
108 three notable changes including Isopropyl  $\beta$ -d-1-thiogalactopyranoside (IPTG)-inducible  
109 *tfoX*, which triggers natural competence, and null mutations in the two nucleases *recJ*  
110 and *exoVII*. *vc1807* is a frame-shifted transposase that appears to be neutral in all  
111 conditions and is used in the MuGENT protocol and thus likely was not responsible for  
112 the lack of growth on TCBS (28). We therefore hypothesized mutation of *tfoX*, *recJ*, or  
113 *exoVII* was responsible for TCBS toxicity. We found that repairing the *tfoX* (strain  
114 CW2171, “+P*tfoX*”) or *recJ* gene (strain CW2173, “+*recJ*”) with WT sequence did not  
115 restore WT-like growth on TCBS agar. However, restoration of the *xseA* null mutation to

116 wild type sequence (strain CW2172, “+*exoVII*”) restored TCBS growth (Fig. 1A). *xseA*,  
117 along with *xseB*, form the ExoVII nuclease that has been implicated in DNA repair. We  
118 thus conclude that *V. cholerae* mutants lacking functional ExoVII are highly attenuated  
119 for growth on TCBS agar.

120

121 We next questioned what component of TCBS agar was responsible for inhibiting the  
122 *exoVII* mutant. TCBS agar contains several selective components that inhibit the growth  
123 of non-*Vibrio* enteric bacteria (Table 1). We retrieved and cultured a mariner transposon  
124 *xseA* mutant (hereafter *xseA*::Tn) from a regenerated ordered *V. cholerae* strain C6706  
125 mutant library (21) and spot plated serial dilutions of this mutant and the WT strain over  
126 different compositions of TCBS agar. As seen with strain E7946, the *xseA* null mutant  
127 of C6706 failed to grow on TCBS (Fig. 1B). We reasoned the non-selective components  
128 of TCBS include sucrose, peptone, yeast extract, and sodium chloride, and media  
129 containing only these four ingredients was termed “TCBS base” media. Alternatively, the  
130 other components of TCBS including sodium citrate, ox bile, sodium cholate, ferric  
131 citrate, and thiosulfate likely provide selection for *Vibrios*. To identify which selective  
132 component of TCBS inhibited growth of the *xseA*::Tn mutant, we spot plated this mutant  
133 and WT on base TCBS containing only one of the selective components. The *xseA*::Tn  
134 mutant grew equivalent to WT in TCBS base agar supplemented with sodium cholate,  
135 sodium citrate, sodium thiosulfate, or ferric citrate added at the wt/vol listed in Table 1,  
136 but was strongly attenuated relative to WT on TCBS base agar supplemented with ox  
137 bile (Fig. 1B). Of note, *xseA*::Tn did exhibit limited growth on ox bile. Thus, we

138 concluded the major selective component responsible for inhibiting the *exoVII* mutant *V.*  
139 *cholerae* strain is ox bile although growth on complete TCBS was the most attenuated.

140

141 ***exoVII* growth inhibition on TCBS can be suppressed by mutations in DNA**

142 **gyrase.** To better understand the requirement for *exoVII* growth on TBCS, we plated the  
143 *xseA::Tn* strain on TCBS agar to select for suppressor mutations that restore growth.

144 We isolated and sequenced the genomes of four suppressor mutants. Three of the four  
145 mutants had unique mutations in either of the two subunits of DNA gyrase- *gyrA* and  
146 *gyrB* (Fig. 2A, Table S1). Of note, one of the four mutants had mutations in both *gyrA*  
147 and *gyrB* (Fig. 2A, Table S1). As DNA gyrase is essential for growth (29–31), we deduce  
148 that these mutations did not produce a null phenotype but rather altered the properties  
149 of DNA gyrase restoring TCBS growth. The suppressor that did not encode a mutation  
150 in *gyrA* or *gyrB* mapped to the ATP-dependent DNA helicase *dinG* (GPY04\_RS07870)  
151 (Table S1), but for this study we will focus on the more common DNA gyrase mutations.  
152 We used MuGENT to regenerate *the gyrA/gyrB* suppressor mutations in the parent  
153 *xseA::Tn* strain and confirmed that promote growth on TCBS agar despite the lack of  
154 functional ExoVII (Fig. 2B).

155

156 ***exoVII* and *gyrAB* alter *V. cholerae* ciprofloxacin resistance.** DNA gyrase, also  
157 known as bacterial type II topoisomerase, relieves topological strain on unwound DNA  
158 by performing negative supercoiling, and is the target of quinolone antibiotics.  
159 Quinolone drugs like ciprofloxacin work as topoisomerase poisons by trapping DNA  
160 gyrase in a covalently attached DNA complex after it makes double stranded breaks

161 (DSBs), causing cell death by inhibiting DNA replication and transcription while leading  
162 to the accumulation of DSBs (32). In *E. coli*, ExoVII mutants are hypersensitive to  
163 ciprofloxacin, and thus ExoVII was hypothesized to relieve covalent complexes of DNA  
164 gyrase bound to DNA (19). To test whether ExoVII has a similar function in *V. cholerae*,  
165 we measured the sensitivity of ExoVII null mutants to ciprofloxacin using a disk diffusion  
166 assay. We found that, indeed, mutant *V. cholerae* lacking either subunit of *exoVII*  
167 (*xseA::Tn* or *xseB::Tn*) are indeed significantly more sensitive to inhibition by  
168 ciprofloxacin than WT exhibiting a larger zone of inhibition (ZOI) (Fig. 3A). We next  
169 hypothesized that suppressor mutations in *gyrA* and/or *gyrB* would reduce ciprofloxacin  
170 sensitivity in the *xseA::Tn* mutant. However, contrary to our prediction only one of the  
171 three suppressor mutant strains (*xseA::Tn gyrB<sub>Δ1018-1026</sub>*) significantly restored WT  
172 ciprofloxacin resistance whereas the other two maintained ciprofloxacin sensitivity  
173 similar to *xseA::Tn* (Fig. 3A). Therefore, even though all three DNA gyrase suppressor  
174 mutants were able to overcome *xseA::Tn* growth inhibition on TCBS, only one leads to  
175 enhanced ciprofloxacin resistance, suggesting that the disruption of DNA gyrase by  
176 TCBS is mechanistically distinct from ciprofloxacin.

177

178 Given that all three sets of DNA gyrase mutations suppress *xseA::Tn* TCBS toxicity but  
179 only one of the three confers ciprofloxacin resistance, we determined if these  
180 suppressor mutations restored growth on bile by plating serial dilutions of the  
181 suppressor mutants on TCBS base agar supplemented with only 0.5% (w/v) ox bile (Fig.  
182 3B). While the *xseA::Tn* and *xseB::Tn* mutants demonstrate strong attenuation when  
183 plated on ox bile, all three suppressor mutants display significantly restored growth



184 although not to the levels observed for WT *V. cholerae*. From these results we conclude  
185 that ox bile induces DNA gyrase-mediated DNA damage, similar to but distinct from  
186 ciprofloxacin, and the ExoVII null mutants fail to grow on TCBS because they are  
187 unable to repair this damage.

188

189 **Passaging *V. cholerae* on TCBS agar selects for ciprofloxacin resistance.** We next  
190 hypothesized that if TCBS and ciprofloxacin inhibit the growth of the *exoVII* mutant via  
191 DNA gyrase toxicity, cells grown on TCBS should be more susceptible to inhibition by  
192 ciprofloxacin than cells grown on LB. We tested this using disc diffusion assays with the  
193 WT strain on LB agar and TCBS agar, and as predicted the zones of inhibition by  
194 ciprofloxacin of cells plated on TCBS agar was significantly greater than that of cells  
195 grown on LB agar (Fig 4A). This suggests that the additional damage caused by TCBS  
196 predisposes *V. cholerae* to ciprofloxacin toxicity. Next, because we found that the  
197 *gyrB*<sub>Δ1018-1026</sub> suppressor mutation increased ciprofloxacin resistance of the *xseA::Tn*  
198 mutant, we tested if this *gyrB* mutations would confer resistance to ciprofloxacin in the  
199 WT strain. Our results demonstrated that the *gyrB*<sub>Δ1018-1026</sub> strain produced a  
200 substantially smaller zone of inhibition than WT, suggesting that this mutant is resistant  
201 to ciprofloxacin even if *xseA* is functional (Fig. 4B).

202

203 Our results thus far suggest that *V. cholerae* growing on TCBS experiences DNA gyrase  
204 mediated DNA damage similar to ciprofloxacin treatment. We therefore tested whether  
205 continuous growth of the WT strain on TCBS agar would impact ciprofloxacin resistance  
206 by serially passaging on either TCBS or LB agar daily for 15 days. Every 3 days we

207 isolated six random clones per lineage to assess their sensitivity to ciprofloxacin by disc  
208 diffusion. On days 12 and 15 we observed an increasingly significant difference in the  
209 distributions of ZOI between the TCBS and LB lineages (Fig. 4C). Notably, while the  
210 TCBS lineage clones varied widely in their sensitivity to ciprofloxacin at every passaging  
211 interval, the LB lineage clones were relatively consistent with the unpassaged  $\Delta lacZ$   
212 parent strain. This result therefore suggests that passaging on TCBS agar potentiates  
213 the evolution of ciprofloxacin resistant *V. cholerae*.

214

215 **Deployment of a randomly-barcoded TnSeq (RB-TnSeq) library identifies DNA**  
216 **repair mutants attenuated for growth on TCBS agar.** Given that our results thus far  
217 suggest TCBS agar causes DNA damage and is selective for *V. cholerae* growth, we  
218 hypothesized that other DNA repair pathways would be required for growth on TCBS  
219 agar. To explore this hypothesis and more generally assess genes necessary for growth  
220 of *V. cholerae* on TCBS, we constructed a randomly barcoded transposon insertion site  
221 sequencing (RB-TnSeq) (23) mutant library in *V. cholerae*. Our library contains over  
222 36,000 barcoded transposon insertion sites mapped to the *V. cholerae* C6706 genome,  
223 with at least one barcoded transposon mapped to 2833/3571 protein-coding genes  
224 (79.33%) (Table 2) (33).

225

226 We first used our RB-TnSeq library in experiments to screen for mutants that failed to  
227 grow. These experiments were done in triplicate in TCBS broth cultures that contained  
228 all components of TCBS (labeled “TCBS complete”) to maintain library diversity. By  
229 sequencing and counting the barcodes present in the selected mutant pool and

230 comparing those counts to those obtained from multiple uncultured library aliquots (see  
231 methods), we calculated scores for 2649 *V. cholerae* genes.

232

233 Our screening approach was validated as we measured highly negative mutant  
234 phenotypes for a multitude of genes that are known to be necessary for survival in the  
235 presence of bile (Fig 5A). For example, the outer membrane porins OmpU and OmpT,  
236 which are known to interact differently with bile, provide a useful test case for the screen  
237 (34). OmpT transport is blocked by deoxycholic acid, and as such does not contribute to  
238 bile resistance (11). The OmpU porin, on the other hand, is transcriptionally upregulated  
239 in response to bile by ToxR and has been long implicated in *V. cholerae* bile resistance  
240 (7, 9). Concordantly, while *ompT* had a nearly neutral score (-0.022) for growth in TCBS  
241 in our screens, *ompU* had a highly negative score (-6.546) (Fig. 5A). We also measured  
242 deleterious phenotypes for mutants in *tolC* (-7.417), *vexAB* (-2.314 and -2.276) and  
243 *vexCD* (-1.98 and -1.914) (Fig. 5A). VexAB and VexCD are Resistance Nodulation  
244 Division (RND) family efflux pumps that function in conjunction with the outer membrane  
245 pore TolC to expel bile acids from the cell and thus, are known to be involved in *V.*  
246 *cholerae* resistance to bile (35–38).

247

248 Given the success of our screen in identifying genes that could be predicted to be  
249 required for growth in TCBS, we next examined the rest of the genome. To identify  
250 genes that are specifically required for TCBS and do not exert general toxicity, we  
251 compared the datasets generated from growth in TCBS broth to a similar analysis of the  
252 library grown in LB using the same conditions. Genes were filtered for specific defects

253 as described in the materials and methods. Filtering the data using these metrics  
254 yielded 111 genes that, when interrupted by Tn insertion, cause strong defects to *V.*  
255 *cholerae* grown in TCBS broth relative to LB (Fig. S1A). Gene ontology term enrichment  
256 analysis using ShinyGO (25) on these 111 genes revealed enrichment for genes  
257 involved in 4 major cellular processes: 1.) phospholipid transport, membrane  
258 organization and lipopolysaccharide (LPS) biosynthesis, 2.) phosphate ion transport, 3.)  
259 DNA replication and repair, and 4.) carbohydrate import and metabolism (Fig. S1B). Of  
260 note, we identified negative scores for many genes implicated in DNA repair (Fig. 5B).  
261 We retrieved several mutants in DNA repair genes from the ordered mutant library and  
262 demonstrated they had decreased growth on TCBS, but not LB, relative to the WT strain  
263 (Fig. 5C).

264

265 **RB-TnSeq reveals both component-dependent and independent growth defects**  
266 **for *V. cholerae* mutants in TCBS.** Given that TCBS is a complex media with many  
267 components (Table 1), we wondered how each selective ingredient impacted the gene  
268 fitness scores observed upon selection with complete TCBS. We once again leveraged  
269 the high-throughput qualities of RB-TnSeq by repeating the TCBS (“complete” medium)  
270 screens in TCBS broth base (“base” medium) and TCBS broth base (“base+1”) media  
271 supplemented with either sodium citrate, ox bile, sodium cholate, ferric citrate, or  
272 sodium thiosulfate (Table 1).

273

274 Principal component analysis of each replicate dataset from both the TCBS complete,  
275 base, and base+1 experiments show strong clustering of replicate experiments (n=3).

276 Interestingly, all the base+1 media datasets cluster together with the exception of base  
277 +ox bile (Fig 6A), demonstrating that the addition of ox bile applies a unique, strong  
278 selective pressure to the pool of mutants relative to the other selective components.  
279 Interestingly, TCBS complete media is distinct from every other dataset, implying that  
280 the multiple inhibitory components in TCBS complete apply a combinatorial selective  
281 pressure on *V. cholerae* growth that cannot be attributed to individual components  
282 themselves.

283

284 Given the observed clustering of the TCBS base +ox bile datasets relative to the rest of  
285 the base+1 experiments, we first examined the results of the TCBS base +ox bile  
286 dataset using the filtering metrics previously described. Filtering genes and scores by  
287 these metrics yielded a list of 60 genes that exhibited specific growth defects in TCBS  
288 base + ox bile (Fig. 6B). As expected, we had strong gene fitness scores for *xseA* and  
289 *xseB* in TCBS complete and TCBS base +ox bile, confirming our previous results (Fig.  
290 6C). Notably, no other strongly negative scores were observed for *xseA* and *xseB* in any  
291 other TCBS base+1 condition, consistent with our results from Fig. 1B. This result  
292 provides confidence that we have captured genuine component-dependent fitness  
293 defects in our barcoded mutant *V. cholerae* strains.

294

295 We next searched for component specific defects by compiling all gene scores across  
296 the TCBS base+1 screens and sorted them by their standard deviation across  
297 conditions, revealing an assortment of genes with highly negative scores in only one or  
298 a few conditions tested (Fig. 6C). *to/C* mutants were highly attenuated in TCBS base

299 supplemented with either ox bile or sodium cholate, but they did not have a fitness  
300 defect in sodium citrate, iron citrate, or sodium thiosulfate. Other genes were specifically  
301 important for growth in sodium cholate (*vexC* and *vexC*) or ox bile (*xseA*, *xseB*, *vexA*,  
302 and *vexB*).

303

304 Additional component-dependent fitness defects were observed for other genes. For  
305 example, transposon mutants in *vc2270* (riboflavin synthase alpha subunit, *ribC*) and  
306 *vc1655* (magnesium transporter, *mgtE*) did not impact growth in bile acids but showed  
307 reduced fitness the base +sodium citrate condition (Fig. 6C). It has been shown  
308 previously that *V. cholerae* lacking the peptidoglycan binding protein *csiV* is  
309 hypersensitive to the bile acid deoxycholate (39). Thus, we were not surprised to find  
310 *csiV* mutants, though selected against in all conditions tested, were most strongly  
311 inhibited by sodium cholate and ox bile. These results demonstrate that each selective  
312 component of TCBS requires a distinct set of genes to allow growth, supporting that  
313 TCBS complete media is the most selective (Fig. 1B) and distinct by PCA analysis (Fig.  
314 6A).

315

## 316 **Discussion**

317 Although TCBS has been used to isolate *V. cholerae* for decades, there is limited  
318 understanding of how this media is selective for *Vibrios* and the traits of *V. cholerae* that  
319 are critical for growth. Here, using a combination of forward and reverse genetics, we  
320 establish that *V. cholerae* experiences significant DNA damage when growing on TCBS  
321 and thus DNA repair is a key phenotype that promotes growth.

322

323 We serendipitously found that ExoVII is necessary for *V. cholerae* growth on TCBS  
324 agar, and that ox bile is largely responsible for the attenuation of *exoVII* mutants.  
325 Additionally, we found that suppression of the *exoVII* TCBS growth defect is through  
326 DNA gyrase mutations. Interestingly, some, but not all, of these DNA gyrase mutations  
327 also confer ciprofloxacin resistance. Previously, ExoVII had no well-described role  
328 outside of functional redundancy with ExoI and SbcCD exonucleases in recombinational  
329 repair (40) and ExoI and RecJ in methyl-directed mismatch repair (MMR) (41). Recently,  
330 ExoVII of *E. coli* was shown to be the exonuclease that is capable of excising  
331 quinolone-induced trapped DNA gyrase cleavage complexes (19). Together, this  
332 evidence suggests that the components of TCBS agar (most likely ox bile) cause  
333 ciprofloxacin like DNA damage to *V. cholerae*, explaining why *exoVII* mutant *V. cholerae*  
334 are inhibited by TCBS.

335

336 We can only speculate how the *gyrA* and *gyrB* mutations suppress the *exoVII* mutant's  
337 sensitivity to ox bile. Even more interesting is the nature of the *gyrB*<sub>Δ1018-1026</sub> mutation  
338 that confers suppression to *exoVII* mutants on TCBS and ciprofloxacin resistance,  
339 considering the most prevalent mechanism for evolving quinolone resistance in bacteria  
340 involves missense mutations in the quinolone resistance determining region (QRDR) of  
341 *gyrA* (amino acids 67-106 according to *E. coli* KL16 numbering) (42, 43). Because these  
342 residues allow targeting of quinolones to DNA gyrase/topoisomerase IV through a  
343 conserved water-metal ion bridge (44, 45), it is unlikely that any of the *gyrA* or *gyrB*  
344 mutations presented here alter the affinity of ciprofloxacin for DNA gyrase. This could

345 indicate that the inhibition of *exoVII* mutant *V. cholerae* on TCBS occurs in a mechanism  
346 distinct from quinolones, though both insults result in lethality due to accumulation of  
347 trapped DNA gyrase cleavage complexes. Further mechanistic studies are required to  
348 disentangle the similarities and differences of how ox bile and ciprofloxacin cause DNA  
349 damage.

350

351 Besides the DNA gyrase mutations, one of the four suppressor mutants was found to  
352 have a frameshift mutation in *dinG* that likely results in a null phenotype. DinG is an  
353 ATP-dependent, structure specific helicase with 5' → 3' directionality (46). *In vitro*  
354 studies using a variety of substrates indicate that DinG is active on structures that mimic  
355 replication and homologous recombination intermediates (47). It has been suggested  
356 that DinG works semi-redundantly alongside helicases Rep and UvrD to permit DNA  
357 replication fork progression through transcribed regions by either displacing R-loops or  
358 dislodging RNA polymerase (48). It is currently unclear why a null mutation in *dinG*  
359 would suppress the toxicity of TCBS to the *exoVII* mutant. However, *dinG* was found to  
360 be upregulated in *E. coli* following treatment with the quinolone nalidixic acid (49).

361 Additionally, *N. meningitidis dinG* mutants were found to be more sensitive to DSBs  
362 caused by mitomycin C than WT (50). We speculate that, in the absence of capable  
363 ExoVII, DinG may be overactive and thus is deleterious for *V. cholerae* cells grown on  
364 TCBS.

365

366 In this work we also confirm that, like in *E. coli* and *S. agalactiae*, *V. cholerae exoVII*  
367 mutants are hypersensitive to ciprofloxacin (19, 51), highlighting a common role for



368 ExoVII in excising quinolone-induced trapped DNA gyrase cleavage complexes among  
369 these bacteria. In doing so we also report a role for ExoVII in surviving bile-mediated  
370 DNA damage. It is of particular interest how ox bile may mimic the DNA-damage caused  
371 by quinolones. An additional complication arises considering that ox bile as a poorly  
372 defined mixture of 9 individual bile acids, with different suppliers having varying  
373 abundances of each bile acid (52).

374

375 It is well understood that bile possesses antimicrobial properties, though our  
376 understanding of the exact mechanism(s) through which killing occurs is incomplete. A  
377 previous study found that the bile acids chenodeoxycholate and deoxycholate activate  
378 the SOS response in *E. coli*. Additionally, the study demonstrates that *E. coli* cells  
379 treated with these bile acids induce the SOS response and are killed similar to  
380 mitomycin C treatment (18). Other studies have suggested roles for base excision  
381 repair, SOS-induced DNA repair, and recombinational repair mediated by RecBCD in *S.*  
382 *enterica* for tolerating bile-induced DNA damage (13, 14). Moreover, evidence from both  
383 gram positive and negative bacteria suggests that resistance to bile is multifaceted.  
384 Several enteric bacteria express efflux pumps capable of expelling bile salts from the  
385 cell, thereby preventing extensive membrane damage caused by the detergent-like  
386 properties of bile. However, when membranes are disrupted and the cell's permeability  
387 barrier is disturbed bile salts may enter cells and cause DNA damage, halting replication  
388 and leading to cell death in the absence of appropriate DNA repair mechanisms (12).

389

390 TCBS is routinely used in laboratories to confirm the identity of *V. cholerae* strains. We  
391 demonstrate here that extended passage of *V. cholerae* on TCBS agar selects for  
392 ciprofloxacin resistant isolates and potentially against mutants that have defects in DNA  
393 repair machinery. Therefore, serial passaging on TCBS might be mutagenic and thus  
394 should be performed cautiously. We suggest against the practice of screening DNA  
395 repair mutant strains over TCBS for confirmation of *Vibrios* since some DNA repair  
396 mutants fail to grow completely and may accumulate further mutations when cultured  
397 over TCBS.

398

399 More importantly, bacterial pathogens can often evolve to have a mutator phenotype  
400 during infection. This is typically a result of deficiencies in MMR (53), and can allow  
401 bacteria to gain genetic diversity to allow rapid evolution to new environments.  
402 Hypermutators have been observed in enteric pathogens like *E. coli* and *S. enteritidis*  
403 (54). Moreover, increased propensity for mutation is likely to play a role in the long-term  
404 colonization of cystic fibrosis (CF) patients, from which hypermutable *Burkholderia*  
405 *pseudomallei* (55), *Haemophilus influenzae* (56) and *Pseudomonas aeruginosa*(57)  
406 have been isolated. For *V. cholerae*, such mutators are not historically thought to evolve  
407 during infection. However, a recent metagenomic study of cholera patients and their  
408 household contacts indicated the presence of hypermutable *V. cholerae* in clinical  
409 isolates from both symptomatic and asymptomatic individuals based on sequence  
410 analysis (58). Our results suggest an intriguing possibility that TCBS itself may be  
411 selecting against mutator strains that evolve *in vivo* leading their underrepresentation in  
412 clinical *V. cholerae* isolates.

413

## 414 **Materials and Methods**

### 415 **Growth of *V. cholerae* strains.**

416 Unless otherwise noted, wild type (WT) and mutant *V. cholerae* strains were cultivated  
417 from frozen glycerol stocks on shaking incubators set to 37°C with shaking at 210rpm.  
418 Strains to be plated in any derivation of TCBS agar were grown in TCBS base broth  
419 (homebrew) using the wt/vol amounts listed in Table 1, while strains plated on LB agar  
420 were grown in LB broth. All strains are described in Table S2 while all primers are  
421 described in Table S3. When necessary, growth media was supplemented with  
422 kanamycin (100 µg/mL), chloramphenicol (10 µg/mL), and/or trimethoprim (10 µg/mL).

423

### 424 **Generation or retrieval of mutant *V. cholerae* strains.**

425 Strain TND0252, TND0252, SAD238 and SAD530 were generously gifted to us by  
426 Ankur Dalia, Indiana University. Strains CW2171, CW2172 and CW2173 were  
427 generated by using natural transformation (MuGENT) as previously described (20).  
428 Briefly, *tfx*, *recJ* and *xseA* genes were amplified from WT C6706 gDNA and then used  
429 to repair these three mutations individually in the TND0252 parent background by co-  
430 transformation with a  $\Delta vc1807::trimR$  fragment. The  $\Delta vc1807::trimR$  fragment was  
431 generated by using primers ABD346 and ABD347 to amplify it from strain SAD530.  
432 Strain JBG013 was made using primers JBG019 and CW2709 to amplify the mutant  
433  $\Delta lacZ$  allele from strain SAD238 (20). We then used MuGENT to transform WT *V.*  
434 *cholerae* with the  $\Delta lacZ$  allele and  $\Delta vc1807::trimR$ , yielding strain JBG013.

435

436 Unless otherwise noted, transposon mutant strains were retrieved from an ordered  
437 mutant library (28). *xseB*::Tn was made by amplifying the region surrounding the *xseB*  
438 locus with primers *xseB\_2.5kb\_F* and *xseB\_2.5kb\_R* (Table S3), and then using an *in*  
439 *vitro* Tn5-Kan<sup>R</sup> transposon insertion kit (Biosearch Technologies Inc, TNP92110).  
440 Competent *V. cholerae* was prepared by growing strain NG001 (harboring plasmid  
441 pMMB-*tfoX-qstR*) in LB broth with chloramphenicol and 100 µg/ml isopropyl β-D-1-  
442 thiogalactopyranoside (IPTG) to maintain the plasmid and induce natural competence,  
443 respectively. Competent NG001 was diluted 1:4 in 0.5x instant ocean before tDNA was  
444 added. We then transformed WT C6706 with the *xseB*::Tn fragment as previously  
445 described (21) and confirmed mutation by sanger sequencing before curing the mutant  
446 of the competence-inducing plasmid.

447

#### 448 **Curing strains of pMMB-*tfoX-qstR*.**

449 Sequence confirmed mutants were isolated and cultured in LB with the appropriate  
450 antibiotic overnight. The following day, the culture was struck over an LB plate to obtain  
451 isolated colonies. After incubation overnight, isolated colonies were selected and patch  
452 plated over LB + kanamycin agar and LB + chloramphenicol agar. Cured clones were  
453 identified as those that grow on LB + kanamycin agar but do not grow on LB +  
454 chloramphenicol agar.

455

#### 456 **Spot plating of bacterial strains.**

457 Strains were grown as previously described overnight before being subcultured 1:100 in  
458 the same medium. Once reaching exponential growth strains were diluted in PBS to an

459 OD<sub>600</sub> of 0.5. Serial 10-fold dilutions were made and 2 µL were plated in spots and  
460 allowed to dry. Plates were then incubated at 37°C overnight.

461

#### 462 **Generation of *xseA::Tn* suppressor mutants.**

463 *xseA::Tn V. cholerae* C6706 was retrieved from an ordered mutant library and cured of  
464 the competence-inducing plasmid (28). *xseA::Tn* was then cultured in LB overnight and  
465 100 µL of the saturated culture was plated on TCBS agar. The plate was incubated at  
466 37°C for 48 hours, after which isolated colonies were selected for follow up  
467 experiments. We extracted genomic DNA from the mutants using the Promega Wizard  
468 Genomic DNA Purification Kit (A1120). Genome sequencing of mutants was performed  
469 by SeqCoast Genomics in 150bp paired-end reads on an Illumina NextSeq 2000 and  
470 mutations were predicted using BreSeq (22).

471

472 Suppressor mutations were determined by comparing the BreSeq outputs for our  
473 evolved suppressor mutants against the BreSeq outputs generated by sequencing an  
474 assortment of repaired ordered library strains. We then amplified the *gyrA* (using  
475 primers *gyrA\_F* and *gyrA\_R*, Table S3) and/or *gyrB* (using primers *gyrB\_F* and *gyrB\_R*,  
476 Table S3) alleles from these mutants and transformed them into either *xseA::Tn* or WT  
477 parent strains using pMMB-*tfoX-qstR* as described above. Mutations were confirmed by  
478 whole genome sequencing before strains were cured of the competence-inducing  
479 plasmid.

480

#### 481 **Disc diffusion assays.**

482 Whatman filter paper was cut into discs using a hole puncher and sterilized by  
483 autoclaving. Strains were grown overnight and then back diluted 1:100 before being  
484 allowed to grow to exponential phase. Cells were then diluted to  $OD_{600}=0.1$  in PBS and  
485 100  $\mu$ L was plated on LB agar or TCBS agar. Discs were then placed with sterile  
486 forceps onto inoculated plates before being impregnated with different dosages of  
487 ciprofloxacin or a 0.1N HCl vehicle control. Plates were incubated at 37°C overnight and  
488 zones of inhibition were measured the following day.

489

#### 490 **Serial passaging over TCBS agar.**

491 A single culture of  $\Delta lacZ$  *V. cholerae* was grown overnight in LB+ trimethoprim. The  
492 following morning the culture was back diluted 1:100 before being allowed to grow to  
493 exponential phase. Cells were then diluted to  $OD_{600}$  to 0.5, and 100  $\mu$ L of diluted culture  
494 was plated on either LB or TCBS agar. Plates were incubated at 37°C overnight. The  
495 following day, a sterile 10  $\mu$ L loop was used to collect samples from bacterial lawns,  
496 which were then resuspended in 10 mL PBS. Samples were then diluted further in PBS  
497 to  $OD_{600}$  of 0.5 and 100  $\mu$ L of the dilutions were replated on either LB or TCBS agar.  
498 Plates were again incubated at 37°C overnight. This process was repeated for 15 days,  
499 with passaging happening once per day per lineage (LB lineage and TCBS lineage).  
500 Every day 1 mL freezer stocks were made from the PBS resuspensions by mixing 750  
501  $\mu$ L with 250  $\mu$ L 80% glycerol and storing at -80°C.

502

503 Every three days, the resuspensions were struck on LB + trimethoprim plates that were  
504 then incubated at 37°C overnight. The following morning, 6 isolated colonies per lineage

505 were picked and cultured in 1mL LB broth at 37°C. Cultures were allowed to grow to  
506 exponential phase, back diluted to OD<sub>600</sub> of 0.1, and 100 µL of each was plated over LB  
507 agar. We then assayed ciprofloxacin sensitivity using the disc diffusion assays  
508 described above.

509

### 510 **Construction and mapping of the RB-TnSeq mutant *V. cholerae* library.**

511 The *E. coli* APA752 donor strain harboring the pKMW3 transposon vector (kindly gifted  
512 to us by Aretha Fiebig, Michigan State University) was grown overnight in LB broth with  
513 0.3 mM diaminopimelic acid (DAP) and kanamycin. We introduced pKMW3 into WT *V.*  
514 *cholerae* through conjugation. The APA752 culture and a WT *V. cholerae* culture were  
515 combined in a 9:1 ratio and before 100 µL was plated over LB with 0.3 mM DAP and  
516 incubated at 37°C overnight. The following day, bacteria were collected with sterile  
517 loops, resuspended in 50 mL LB, and pelleted by centrifugation. The supernatant was  
518 removed, and cells were washed in 15 mL LB to remove residual DAP. 5 mL of 80%  
519 glycerol was added, and the entire 20 mL volume was split up between 10x2 mL frozen  
520 stocks. Transposon mutant titer was measured by plating transconjugants over LB +  
521 kanamycin agar. Afterwards, 200 µL of thawed transconjugant stocks were plated over  
522 twenty-five 150x15mm petri dishes containing LB agar with kanamycin. Plates were  
523 incubated at 37°C for 48 hours.

524

525 Following incubation, three representative plates were selected, and colonies were  
526 counted to estimate the total mutant colonies collected between all 25 plates. For each  
527 plate, 3 mL of LB was added, and colonies were resuspended using sterile L-shaped

528 spreaders. We collected as much of the 3 mL volume as possible from each plate and  
529 pooled it all in a single 50 mL conical. Afterwards, 30 mL of the collected cells were  
530 added to a flask containing 270 mL LB with kanamycin, and the mutants were incubated  
531 at 37°C with 210 rpm shaking for 1 hour. Glycerol was then added to a 20% final  
532 concentration and hundreds of 100 µL library aliquots were frozen for single use, as well  
533 as a few dozen 1mL aliquots to facilitate efficient genomic DNA extraction. We extracted  
534 genomic DNA from the mutants using the Promega Wizard Genomic DNA Purification  
535 Kit.

536  
537 For library mapping, we followed the strategy of Wetmore and colleagues (23) with  
538 minor modifications to the PCR enrichment of barcode-containing insertion junctions.  
539 The modifications are described in detail elsewhere (24). Briefly, 5 µg of library genomic  
540 DNA was sheared with a Covaris M220 ultrasonicator to produce ~300 bp fragments.  
541 Genomic DNA was then electrophoresed on a 1% TBE gel, stained with SYBR Gold  
542 (Invitrogen, S11494), and gel extracted using the Zymoclean Gel DNA Recovery Kit  
543 (Zymo Research, D4001) to select for fragments between 150-500 bp. We then  
544 performed end repair, A-tailing and adaptor ligation with the NEBNext Ultra II DNA  
545 Library Prep Kit for Illumina (E7645S) following the manufacturer's recommended  
546 protocol using custom adaptors made by annealing oligos Mod2\_Truseq and  
547 Mod2\_TS\_Univ (Table S3). Adaptor-ligated DNA was cleaned without size selection  
548 using NEBNext Sample Purification Beads (0.9x) and eluted in 0.1x TE buffer following  
549 the manufacturer's instructions.

550



551 DNA fragments containing the transposons were enriched in a 2-step nested PCR  
552 strategy using modified primer sequences based on the original primer sequences used  
553 by Wetmore et al (23). This modified enrichment strategy is described by Fiebig and  
554 colleagues (24). In the first PCR we used the forward primer TS\_pHimar+4\_F and the  
555 reverse primer TS\_R (Table S3). Cycling parameters were 98°C for 2 min, 10x (98°C,  
556 30sec; 70°C, 20sec; 72°C, 20sec), 72°C for 5min, and a 4°C hold. After the first PCR,  
557 products were cleaned again using NEBNext Sample Purification beads (0.9x) and  
558 eluted in 0.1x TE buffer. 15 µL of the cleaned PCR product was used as template in the  
559 second transposon enriching PCR. In the second PCR we used the primers  
560 P7\_MOD\_TS\_index3 and P5\_TS\_F (Table S3) to add Illumina P5 and P7 sequences  
561 and a 6-bp i7 index. Cycling parameters were 98°C for 3 min, 10x (98°C, 20sec; 70°C,  
562 10sec; 72°C, 20sec), 72°C for 5min, and a 4°C hold. Following the second PCR,  
563 products were again cleaned using NEBNext Sample Purification beads (0.9x) and  
564 eluted in 0.1x TE buffer. Reagents for both PCR reactions were supplied in the  
565 NEBNext Ultra II DNA Library Prep Kit for Illumina. For both reactions we used the  
566 volumes of reagents as outlined by the kit manual. Prepared reads were submitted to  
567 SeqCoast Genomics (Portsmouth, NH) for sequencing on an Illumina NextSeq using a  
568 300-cycle NextSeq P1 reagent kit (Illumina 20050264). The sequencing run was  
569 supplemented with 25% phiX DNA to aid in clustering. Locations of reliable transposon  
570 insertions were aligned and mapped to the *V. cholerae* C6706 genome (GenBank  
571 accession numbers CP064350 and CP064351) using custom Perl scripts written and  
572 described by Wetmore et al (23) (available at

573 <https://bitbucket.org/berkeleylab/feba/src/master/>). Mapping statistics are provided in  
574 Table 2.

575

576 **Competition of RB-TnSeq *V. cholerae* mutants in liquid media.**

577 For each replicate RB-TnSeq experiment in TCBS broth (including TCBS with or without  
578 a selective component), we thawed a single 100  $\mu$ L aliquot of the RB-TnSeq library on  
579 ice before being added to 100 mL of experimental liquid medium in 250 mL unbaffled  
580 Erlenmeyer flasks. Initial OD<sub>600</sub> values were obtained before cultures were incubated for  
581 5 hours at 37°C with shaking. OD<sub>600</sub> values were taken hourly. After 5 hours, cultures  
582 were collected in 50 mL conical tubes and pelleted. Supernatants were removed and  
583 genomic DNA was extracted from pellets as described above. The comparison  
584 experiment performed in LB broth was done almost exactly as described above, except  
585 that the cultures were incubated until they had reached OD<sub>600</sub> of ~1.0 (4 hours and 10  
586 minutes)

587

588 The amplification and sequencing of barcodes was performed following the approach  
589 described by Wetmore et al (23). 100-200 ng of genomic DNA from each experiment  
590 sample was used as template to amplify mutant barcodes by PCR. Barcodes were  
591 amplified in 50  $\mu$ L reaction volumes using Q5 DNA polymerase (New England Biolabs)  
592 using 1x Q5 reaction buffer, 1x High GC enhancer, 1.0 units Q5 polymerase, 0.2 mM  
593 dNTP and 0.4  $\mu$ M of each primer. The forward primer was BarSeq\_P1, while each  
594 reaction used a uniquely indexed reverse primer BarSeq\_P2\_ITXXX, where “XXX”  
595 corresponds to the index number as used by Wetmore and colleagues (Table S3).

596 Reaction conditions were as follows: 98°C for 4 min, 25x (98°C, 30sec; 55°C, 30sec;  
597 72°C, 30sec), 72°C for 5min, and a 4°C hold. Following, samples were run on a 2% TAE  
598 agarose gel to confirm the presence of PCR products. 5 µL of each PCR was then  
599 pooled, and the pool of PCR products was cleaned using a DNA Clean & Concentrator  
600 kit (Zymo Research, D4003).

601  
602 Barcodes were then sequenced by SeqCenter (Pittsburgh, PA) on a single lane of a  
603 NovaSeq X Plus flowcell in 2x150-cycle configuration. Barcodes were supplemented  
604 with 50% phiX DNA to aid in clustering and loaded at 110 pM. Reads were trimmed to  
605 75 bp before analysis to eliminate unnecessary Illumina adaptors, leaving the barcode  
606 sequence. Barcode sequences in each sample were counted and the fitness of each  
607 mutant strain was calculated as the normalized log<sub>2</sub> difference in barcode counts in the  
608 treated sample versus replicate reference samples using the custom scripts developed  
609 by Wetmore et al. For our reference samples, we extracted genomic DNA from four  
610 individual uncultured 100 µL library aliquots, amplified the barcodes and sequenced  
611 them as described above. Gene scores were calculated based on the weighted average  
612 of strain scores for mutants with insertions in the central 80% coding region of the gene,  
613 again using the scripts developed by Wetmore et al. (available at  
614 <https://bitbucket.org/berkeleylab/feba/src/master/>).

615

### 616 **Gene Ontology enrichment using ShinyGO.**

617 We wanted to identify genes that were specifically important for TCBS growth and not  
618 standard rich media. To identify these genes, we made the following comparison of

619 fitness scores in TCBS to those in LB. Having calculated gene scores based on  
620 differences in barcode abundance relative to an uncultured library sample, we then  
621 filtered our analysis to exclude genes that have a score in TCBS or TCBS base +ox bile  
622  $\leq -1$  (mutant must be attenuated for growth in the experimental condition),  $\geq -2$  in LB (to  
623 exclude those mutants with general fitness defects in rich media), and a difference in  
624 scores between the two conditions (experimental condition score – LB score)  $\leq -1$ . Using  
625 this thresholding strategy, we identified 111 genes necessary for growth in TCBS broth  
626 and 60 genes necessary for growth in TCBS base + ox bile broth, relative to their  
627 necessity for growth in LB.

628

629 We then performed gene ontology enrichment by comparing the gene IDs against  
630 annotations present in the *V. cholerae* N16961 genome (taxonomy ID 243277) using  
631 ShinyGO 0.80 (25). To eliminate error in the false discovery rate produced by ShinyGO,  
632 we submitted a background list of genes that included the gene IDs for all 2649 scored  
633 across the RB-TnSeq experiments. This way, enrichment of genes meeting our filtering  
634 criteria isn't biased by the absence of genes we were unable to assign scores to in our  
635 RB-TnSeq experiments. ShinyGO options were as follows: FDR cutoff = 0.05, #  
636 pathways to show = 10, pathway size minimum = 10. For clarity, we then performed  
637 some manual binning of pathways based on redundancy between pathway names and  
638 the genes belonging to them (for example, pathways “DNA replication, and DNA repair”,  
639 “DNA metabolic process, and chromosome segregation” and “DNA repair, and DNA-  
640 dependent ATPase activity” contain many of the same genes, so we group them  
641 together more broadly under “DNA repair”).

642

643 **Statistical analysis and data visualization.**

644 All statistical analyses were performed in GraphPad Prism version 10.1.1 Principal  
645 component analysis plot was made in R version 4.3.2 (26) using the vegan package  
646 (27) version 2.6-6.1.

647

648 **ACKNOWLEDGEMENTS**

649 This research was supported and funded by NIH grants GM139537 and AI158433 to  
650 C.M.W. We thank Jasper Gomez for constructing strain JBG013. We also thank Aretha  
651 Fiebig for sharing the strain and expertise necessary for generating the *V. cholerae* RB-  
652 TnSeq library and Ankur Dalia for sharing strains.

653

- 654 1. Charnley GEC, Kelman I, Murray KA. 2021. Drought-related cholera outbreaks in  
655 Africa and the implications for climate change: a narrative review. *Pathog Glob*  
656 *Health* 116:3–12: <https://doi.org/10.1080/20477724.2021.1981716>.  
657
- 658 2. Montero DA, Vidal RM, Velasco J, George S, Lucero Y, Gómez LA, Carreño LJ,  
659 García-Betancourt R, O’Ryan M. 2023. *Vibrio cholerae*, classification,  
660 pathogenesis, immune response, and trends in vaccine development. *Front Med*  
661 (Lausanne) 10: <https://doi.org/10.3389/fmed.2023.1155751>.  
662
- 663 3. Ramamurthy T, Das B, Chakraborty S, Mukhopadhyay AK, Sack DA. 2020.  
664 Diagnostic techniques for rapid detection of *Vibrio cholerae* O1/O139. *Vaccine*  
665 38:A73–A82: <https://doi.org/10.1016/j.vaccine.2019.07.099>.  
666
- 667 4. Janda JM, Powers C, Bryant RG, Abbott SL. 1988. Current Perspectives on the  
668 Epidemiology and Pathogenesis of Clinically Significant *Vibrio* spp. *Clin Microbiol*  
669 *Rev* 1:245–267.  
670
- 671 5. Gubensäk N, Sagmeister T, Buhlheller C, Geronimo BD, Wagner GE, Petrowitsch  
672 L, Gräwert M, Rotzinger M, Berger TMI, Schäfer J, Usón I, Reidl J, Sánchez-  
673 Murcia PA, Zangger K, Pavkov-Keller T. 2023. *Vibrio cholerae*’s ToxRS Bile  
674 Sensing System. *Elife* 12: <https://doi.org/10.7554/eLife.88721>.  
675

- 676 6. Bina TF, Kunkle DE, Renee Bina X, Mullett SJ, Wendell SG, Bina JE. 2021. Bile  
677 Salts Promote ToxR Regulon Activation during Growth under Virulence-Inducing  
678 Conditions. *Infect Immun* 89: <https://doi.org/10.1128/IAI>.  
679
- 680 7. Provenzano D, Klose KE. 2000. Altered expression of the ToxR-regulated porins  
681 OmpU and OmpT diminishes *Vibrio cholerae* bile resistance, virulence factor  
682 expression, and intestinal colonization. *PNAS* 97:10220–10224.  
683
- 684 8. Provenzano D, Lauriano CM, Klose KE. 2001. Characterization of the role of the  
685 ToxR-modulated outer membrane porins OmpU and OmpT in *Vibrio cholerae*  
686 virulence. *J Bacteriol* 183:3652–3662: [https://doi.org/10.1128/JB.183.12.3652-](https://doi.org/10.1128/JB.183.12.3652-3662.2001)  
687 [3662.2001](https://doi.org/10.1128/JB.183.12.3652-3662.2001).  
688
- 689 9. Provenzano D, Schuhmacher DA, Barker JL, Klose KE. 2000. The Virulence  
690 Regulatory Protein ToxR Mediates Enhanced Bile Resistance in *Vibrio cholerae*  
691 and Other Pathogenic *Vibrio* Species. *Infect Immun* 68:1491–1497.  
692
- 693 10. Simonet VC, Baslé A, Klose KE, Delcour AH. 2003. The *Vibrio cholerae* porins  
694 OmpU and OmpT have distinct channel properties. *Journal of Biological*  
695 *Chemistry* 278:17539–17545: <https://doi.org/10.1074/jbc.M301202200>.  
696
- 697 11. Duret G, Delcour AH. 2006. Deoxycholic acid blocks *Vibrio cholerae* OmpT but  
698 not OmpU porin. *Journal of Biological Chemistry* 281:19899–19905:  
699 <https://doi.org/10.1074/jbc.M602426200>.  
700
- 701 12. Merritt ME, Donaldson JR. 2009. Effect of bile salts on the DNA and membrane  
702 integrity of enteric bacteria. *J Med Microbiol* 58:1533–1541:  
703 <https://doi.org/10.1099/jmm.0.014092-0>.  
704
- 705 13. Prieto AI, Ramos-Morales F, Casadesús J. 2006. Repair of DNA damage induced  
706 by bile salts in *Salmonella enterica*. *Genetics* 174:575–584:  
707 <https://doi.org/10.1534/genetics.106.060889>.  
708
- 709 14. Prieto AI, Ramos-Morales F, Casadesús J. 2004. Bile-induced DNA damage in  
710 *Salmonella enterica*. *Genetics* 168:1787–1794:  
711 <https://doi.org/10.1534/genetics.104.031062>.  
712
- 713 15. Rincé A, Le Breton Y, Verneuil N, Giard JC, Hartke A, Auffray Y. 2003.  
714 Physiological and molecular aspects of bile salt response in *Enterococcus*  
715 *faecalis*. *Int J Food Microbiol* 88:207–213: [https://doi.org/10.1016/S0168-](https://doi.org/10.1016/S0168-1605(03)00182-X)  
716 [1605\(03\)00182-X](https://doi.org/10.1016/S0168-1605(03)00182-X).  
717
- 718 16. Ruiz L, Sánchez B, Ruas-Madiedo P, De Los Reyes-Gavilán CG, Margolles A.  
719 2007. Cell envelope changes in *Bifidobacterium animalis* ssp. *lactis* as a response  
720 to bile. *FEMS Microbiol Lett* 274:316–322: [https://doi.org/10.1111/j.1574-](https://doi.org/10.1111/j.1574-6968.2007.00854.x)  
721 [6968.2007.00854.x](https://doi.org/10.1111/j.1574-6968.2007.00854.x).



- 722  
723 17. Ruiz L, Couté Y, Sánchez B, De los Reyes-Gavilán CG, Sanchez JC, Margolles A.  
724 2009. The cell-envelope proteome of *Bifidobacterium longum* in an in vitro bile  
725 environment. *Microbiology (N Y)* 155:957–967:  
726 <https://doi.org/10.1099/mic.0.024273-0>.  
727
- 728 18. Kandell RL, Bernstein C. 1991. Bile Salt/Acid Induction of DNA Damage in  
729 Bacterial and Mammalian Cells: Implications for Colon Cancer. *Nutr Cancer*  
730 16:227–238: <https://doi.org/10.1080/01635589109514161>.  
731
- 732 19. Huang SN, Michaels SA, Mitchell BB, Majdalani N, Broeck AV, Canela A, Tse-Dinh  
733 YC, Lamour V, Pommier Y. 2021. Exo7 resolves DNA gyrase cleavage  
734 complexes. *Sci Adv* 10:1–10: <https://doi.org/10.1126/sciadv.abe0384>.  
735
- 736 20. Dalia AB, McDonough EK, Camilli A. 2014. Multiplex genome editing by natural  
737 transformation. *Proc Natl Acad Sci U S A* 111:8937–8942:  
738 <https://doi.org/10.1073/pnas.1406478111>.  
739
- 740 21. Grant NA, Donkor GY, Sontz JT, Soto W, Waters CM. 2024. Deployment of a  
741 *Vibrio cholerae* ordered transposon mutant library in a quorum-competent genetic  
742 background. *bioRxiv* <https://doi.org/10.1101/2023.10.31.564941>.  
743
- 744 22. Barrick JE, Colburn G, Deatherage DE, Traverse CC, Strand MD, Borges JJ,  
745 Knoester DB, Reba A, Meyer AG. 2014. Identifying structural variation in haploid  
746 microbial genomes from short-read resequencing data using breseq. *BMC*  
747 *Genomics* 15: <https://doi.org/10.1186/1471-2164-15-1039>.  
748
- 749 23. Wetmore KM, Price MN, Waters RJ, Lamson JS, He J, Hoover CA, Blow MJ,  
750 Bristow J, Butland G, Arkin AP, Deutschbauer A. 2015. Rapid quantification of  
751 mutant fitness in diverse bacteria by sequencing randomly bar-coded  
752 transposons. *mBio* 6:1–15: <https://doi.org/10.1128/mBio.00306-15>.  
753
- 754 24. Fiebig A, Schnizlein MK, Pena-Rivera S, Trigodet F, Dubey AA, Hennessy MK,  
755 Basu A, Pott S, Dalal S, Rubin D, Sogin ML, Eren AM, Chang EB, Crosson S.  
756 2024. Bile acid fitness determinants of a *Bacteroides fragilis* isolate from a human  
757 pouchitis patient. *mBio* 15: <https://doi.org/10.1128/mbio.02830-23>.  
758
- 759 25. Xijin Ge S, Jung D, Yao R. 2019. ShinyGO: a graphical gene-set enrichment tool  
760 for animals and plants. *Bioinformatics* 8:2628–2629:  
761 <https://doi.org/10.5281/zenodo.1451847>.  
762
- 763 26. R Core Team. 2023. R: A Language and Environment for Statistical Computing. R  
764 Foundation for Statistical Computing.  
765
- 766 27. Oksanen J, Simpson GL, Blanchet FG, Kindt R, Legendre P, Minchin PR, O'Hara  
767 R, Solymos P, Stevens M, Szoecs E, Wagner H, Barbour M, Bedward M, Bolker

- 768 B, Borcard D, Borman T, Carvalho G, Chirico M, De Caceres M, Durand S,  
769 Evangelista H, FitzJohn R, Friendly M, Furneaux B, Hannigan G, Hill M, Lahti L,  
770 McGlenn D, Ouellette M, Ribeiro Cunha E, Smith T, Stier A, Ter Braak C, Weedon  
771 J. 2024. vegan: Community Ecology Package. R package version 2.6-6.1.  
772
- 773 28. Dalia TN, Yoon SH, Galli E, Barre FX, Waters CM, Dalia AB. 2017. Enhancing  
774 multiplex genome editing by natural transformation (MuGENT) via inactivation of  
775 ssDNA exonucleases. *Nucleic Acids Res* 45:7527–7537:  
776 <https://doi.org/10.1093/nar/gkx496>.  
777
- 778 29. Kreuzer KN, McEntee K, Geballe AP, Cozzarelli NR. 1978. Lambda Transducing  
779 Phages for the *nalA* Gene of *Escherichia coli* and Conditional Lethal *nalA*  
780 Mutations 167:129–137.  
781
- 782 30. Steck TF, Drlica K. 1984. Bacterial Chromosome Segregation: Evidence for DNA  
783 Gyrase Involvement in Decatenation. *Cell* 36:1081–1088.  
784
- 785 31. Gerdes SY, Scholle MD, Campbell JW, Balázsi G, Ravasz E, Daugherty MD,  
786 Somera AL, Kyrpides NC, Anderson I, Gelfand MS, Bhattacharya A, Kapatral V,  
787 D'Souza M, Baev M V., Grechkin Y, Mseeh F, Fonstein MY, Overbeek R, Barabási  
788 AL, Oltvai ZN, Osterman AL. 2003. Experimental determination and system level  
789 analysis of essential genes in *Escherichia coli* MG1655. *J Bacteriol* 185:5673–  
790 5684: <https://doi.org/10.1128/JB.185.19.5673-5684.2003>.  
791
- 792 32. Bush NG, Diez-Santos I, Abbott LR, Maxwell A. 2020. Quinolones: Mechanism,  
793 lethality and their contributions to antibiotic resistance. *Molecules* 25:  
794 <https://doi.org/10.3390/molecules25235662>.  
795
- 796 33. Yuding Weng, Renee Bina, James E. Bina. 2021. Complete Genome Sequence  
797 of *Vibrio cholerae* O1 El Tor Strain C6706. *Microbiol Resour Announc* 10:1–2:  
798 <https://doi.org/10.1128/CMR.8.1.48>.  
799
- 800 34. Wibbenmeyer JA, Provenzano D, Landry CF, Klose KE, Delcour AH. 2002. *Vibrio*  
801 *cholerae* OmpU and OmpT porins are differentially affected by bile. *Infect Immun*  
802 70:121–126: <https://doi.org/10.1128/IAI.70.1.121-126.2002>.  
803
- 804 35. Bina JE, Mekalanos JJ. 2001. *Vibrio cholerae toIC* is required for bile resistance  
805 and colonization. *Infect Immun* 69:4681–4685:  
806 <https://doi.org/10.1128/IAI.69.7.4681-4685.2001>.  
807
- 808 36. Bina XR, Provenzano D, Nguyen N, Bina JE. 2008. *Vibrio cholerae* RND family  
809 efflux systems are required for antimicrobial resistance, optimal virulence factor  
810 production, and colonization of the infant mouse small intestine. *Infect Immun*  
811 76:3595–3605: <https://doi.org/10.1128/IAI.01620-07>.  
812



- 813 37. Bina XR, Bina JE. 2023. *Vibrio cholerae* RND efflux systems: mediators of stress  
814 responses, colonization and pathogenesis. *Front Cell Infect Microbiol* 13:  
815 <https://doi.org/10.3389/fcimb.2023.1203487>.  
816
- 817 38. Bina JE, Provenzano D, Wang C, Bina XR, Mekalanos JJ. 2006. Characterization  
818 of the *Vibrio cholerae* *vexAB* and *vexCD* efflux systems. *Arch Microbiol* 186:171–  
819 181: <https://doi.org/10.1007/s00203-006-0133-5>.  
820
- 821 39. Dörr T, Lam H, Alvarez L, Cava F, Davis BM, Waldor MK. 2014. A Novel  
822 Peptidoglycan Binding Protein Crucial for PBP1A-Mediated Cell Wall Biogenesis  
823 in *Vibrio cholerae*. *PLoS Genet* 10: <https://doi.org/10.1371/journal.pgen.1004433>.  
824
- 825 40. Repar J, Briški N, Buljubašić M, Zahradka K, Zahradka D. 2013. Exonuclease VII  
826 is involved in “reckless” DNA degradation in UV-irradiated *Escherichia coli*. *Mutat*  
827 *Res Genet Toxicol Environ Mutagen* 750:96–104:  
828 <https://doi.org/10.1016/j.mrgentox.2012.10.005>.  
829
- 830 41. Burdett V, Baitinger C, Viswanathan M, Lovett ST, Modrich P. 2001. In vivo  
831 requirement for RecJ, ExoVII, ExoI, and ExoX in methyl-directed mismatch repair.  
832 *PNAS* 98:6765: <https://doi.org/https://doi.org/10.1073/pnas.121183298>.  
833
- 834 42. Yoshida H, Bogaki M, Nakamura M, Nakamura S. 1990. Quinolone Resistance-  
835 Determining Region in the DNA Gyrase *gyrA* Gene of *Escherichia coli*. *Antimicrob*  
836 *Agents Chemother* 1271–1272.  
837
- 838 43. Aldred KJ, Kerns RJ, Osheroff N. 2014. Mechanism of quinolone action and  
839 resistance. *Biochemistry* 53:1565–1574: <https://doi.org/10.1021/bi5000564>.  
840
- 841 44. Aldred KJ, McPherson SA, Turnbough CL, Kerns RJ, Osheroff N. 2013.  
842 Topoisomerase IV-quinolone interactions are mediated through a water-metal ion  
843 bridge: Mechanistic basis of quinolone resistance. *Nucleic Acids Res* 41:4628–  
844 4639: <https://doi.org/10.1093/nar/gkt124>.  
845
- 846 45. Wohlkonig A, Chan PF, Fosberry AP, Homes P, Huang J, Kranz M, Leydon VR,  
847 Miles TJ, Pearson ND, Perera RL, Shillings AJ, Gwynn MN, Bax BD. 2010.  
848 Structural basis of quinolone inhibition of type IIA topoisomerases and target-  
849 mediated resistance. *Nat Struct Mol Biol* 17:1152–1153:  
850 <https://doi.org/10.1038/nsmb.1892>.  
851
- 852 46. Voloshin ON, Vanevski F, Khil PP, Camerini-Otero RD. 2003. Characterization of  
853 the DNA damage-inducible helicase DinG from *Escherichia coli*. *Journal of*  
854 *Biological Chemistry* 278:28284–28293: <https://doi.org/10.1074/jbc.M301188200>.  
855
- 856 47. Voloshin ON, Camerini-Otero RD. 2007. The DinG protein from *Escherichia coli* is  
857 a structure-specific helicase. *Journal of Biological Chemistry* 282:18437–18447:  
858 <https://doi.org/10.1074/jbc.M700376200>.

- 859  
860 48. Boubakri H, De Septenville AL, Viguera E, Michel B. 2010. The helicases DinG,  
861 Rep and UvrD cooperate to promote replication across transcription units in vivo.  
862 EMBO Journal 29:145–157: <https://doi.org/10.1038/emboj.2009.308>.  
863
- 864 49. Van Dyk TK, DeRose EJ, Gonye GE. 2001. LuxArray, a high-density, genomewide  
865 transcription analysis of *Escherichia coli* using bioluminescent reporter strains. J  
866 Bacteriol 183:5496–5505: <https://doi.org/10.1128/JB.183.19.5496-5505.2001>.  
867
- 868 50. Frye SA, Beyene GT, Namouchi A, Gómez-Muñoz M, Homberset H, Kalayou S,  
869 Riaz T, Tønjum T, Balasingham S V. 2017. The helicase DinG responds to stress  
870 due to DNA double strand breaks. PLoS One 12:  
871 <https://doi.org/10.1371/journal.pone.0187900>.  
872
- 873 51. Briaud P, Gautier T, Rong V, Mereghetti L, Lanotte P, Hiron A. 2023. The  
874 *Streptococcus agalactiae* Exonuclease ExoVII Is Required for Resistance to  
875 Exogenous DNA-Damaging Agents. J Bacteriol 205:  
876 <https://doi.org/10.1128/jb.00024-23>.  
877
- 878 52. Hu PL, Yuan YH, Yue TL, Guo CF. 2018. Bile acid patterns in commercially  
879 available oxgall powders used for the evaluation of the bile tolerance ability of  
880 potential probiotics. PLoS One 13: <https://doi.org/10.1371/journal.pone.0192964>.  
881
- 882 53. Jolivet-Gougeon A, Kovacs B, Le Gall-David SL, Le Bars H, Bousarghin L,  
883 Bonnaure-Mallet M, Lobe B, Guillé F, Soussy CJ, Tenke P. 2011. Bacterial  
884 hypermutation: Clinical implications. J Med Microbiol 60:563–573:  
885 <https://doi.org/10.1099/jmm.0.024083-0>.  
886
- 887 54. Leclerc JE, Li B, Payne WL, Cebula TA. 1996. High Mutation Frequencies Among  
888 *Escherichia coli* and *Salmonella* Pathogens. New Series 274:1208–1211:  
889 <https://doi.org/DOI:10.1126/science.274.5290.1208>.  
890
- 891 55. Viberg LT, Sarovich DS, Kidd TJ, Geake JB, Bell SC, Currie BJ, Price EP. 2017.  
892 Within-host evolution of *Burkholderia Pseudomallei* during chronic infection of  
893 seven Australasian cystic fibrosis patients. mBio 8:  
894 <https://doi.org/10.1128/mBio.00356-17>.  
895
- 896 56. Watson ME, Burns JL, Smith AL. 2004. Hypermutable *Haemophilus influenzae*  
897 with mutations in *mutS* are found in cystic fibrosis sputum. Microbiology (N Y)  
898 150:2947–2958: <https://doi.org/10.1099/mic.0.27230-0>.  
899
- 900 57. Mena A, Smith EE, Burns JL, Speert DP, Moskowitz SM, Perez JL, Oliver A. 2008.  
901 Genetic adaptation of *Pseudomonas aeruginosa* to the airways of cystic fibrosis  
902 patients is catalyzed by hypermutation. J Bacteriol 190:7910–7917:  
903 <https://doi.org/10.1128/JB.01147-08>.  
904

905 58. Levade I, Khan AI, Chowdhury F, Calderwood SB, Ryan ET, Harris JB, LaRocque  
906 RC, Bhuiyan TR, Qadri F, Weil AA, Shapiro BJ. 2021. A Combination of  
907 Metagenomic and Cultivation Approaches Reveals Hypermutator Phenotypes  
908 within *Vibrio cholerae*-Infected Patients. *mSystems* 6:  
909 <https://doi.org/10.1128/msystems.00889-21>.  
910

911

912

### 913 **FIGURE LEGENDS**

914 **Figure 1: *exoVII* mutant *V. cholerae* cannot grow on TCBS agar.** (A) Parent strains  
915 (left plate) and repaired strains (right plate) were struck over TCBS agar and assayed  
916 for growth after 24 hours incubation. Strain E7946 is the parent to TND0252. TND0252  
917 is the parent strain to CW2171, CW2172 and CW2173. (B) Serial dilutions of WT and  
918 *xseA::Tn V. cholerae* spotted over TCBS agar, or TCBS base agar supplemented with a  
919 single selective component as indicated using the wt/vol listed in Table 1. For both  
920 figures A and B, plates shown are representative of 3 biological replicate experiments.

921

922 **Figure 2: Inhibition of *exoVII* mutants on TCBS agar can be suppressed by**  
923 **mutations in DNA gyrase.** (A) Together, *gyrA* and *gyrB* encode DNA gyrase. Color-  
924 coded bands within the *gyrA* and *gyrB* reading frames correspond to mutations present  
925 among three suppressor mutants generated by plating *xseA::Tn* over TCBS agar and  
926 selecting isolated colonies once growth was observed. (B) Serial dilution and spot  
927 plating of WT, *xseA::Tn* and *exoVII* suppressor mutants over TCBS agar and LB agar.  
928 Plates shown are representative of 3 biological replicate experiments.

929

930 **Figure 3: *exoVII* and *gyrAB* alter *V. cholerae* ciprofloxacin resistance.** (A) WT,  
931 *exoVII* and *exoVII* suppressor mutants were assayed for ciprofloxacin sensitivity by disc  
932 diffusion with 5 ng of ciprofloxacin on LB agar. Results shown are from 6 biological  
933 replicate experiments. The dotted line at 6mm is labeled “LOD” for limit of detection as  
934 discs were 6 mm in diameter. Results were analyzed by one-way repeated measures  
935 ANOVA with Bonferroni’s multiple comparisons test. ns,  $P > 0.05$ ; \*,  $P \leq 0.05$ ; \*\*,  $P \leq$   
936  $0.01$ ; \*\*\*,  $P \leq 0.001$ . (B) Serial dilution and spot plating of WT, *exoVII* and *exoVII*  
937 suppressor mutants over TCBS base + ox bile agar. Plates shown are representative of  
938 3 biological replicate experiments.

939

940 **Figure 4: Passaging *V. cholerae* on TCBS agar selects for ciprofloxacin**  
941 **resistance.** (A) WT *V. cholerae* was assayed for ciprofloxacin sensitivity by disc  
942 diffusion with 5ng of ciprofloxacin on LB or TCBS agar. Results shown are from 6  
943 biological replicate experiments. Results were analyzed by unpaired T test using the  
944 Holm-Sidak method.  $P < 0.0001$ . (B) WT *V. cholerae* and a strain carrying the *gyrB* <sub>$\Delta$ 1018-</sub>  
945 <sub>1026</sub> mutation were assayed for ciprofloxacin sensitivity by disc diffusion with 5ng of  
946 ciprofloxacin on LB agar. Results shown are from 6 biological replicate experiments.  
947 Results were analyzed by unpaired T test with Welch correction using the Holm-Sidak  
948 method.  $P < 0.0001$ . (C) Comparison of ciprofloxacin sensitivity of 6 randomly-selected  
949 isolated *V. cholerae* (*lacZ* mutant) colonies following consecutive daily passages on  
950 either TCBS or LB agar (see methods). Isolates were assayed for ciprofloxacin  
951 sensitivity by disc diffusion with 5ng of ciprofloxacin on LB agar. The red lines  
952 correspond to the median ZOI among the 6 isolates. The dashed lines labeled “*lacZ*”

953 and “WT” represent the average ( $n = 3$ ) ZOIs for the unpassaged *lacZ* parent strain and  
954 unpassaged WT *V. cholerae*, respectively. Each data point represents the ZOI of a  
955 distinct isolate. Results were analyzed by Mann-Whitney two-tailed T test between the  
956 two lineages at each passage shown. Day 12,  $P = 0.026$ ; Day 15,  $P = 0.0087$ . In A, B  
957 and C, the dotted line at 6mm is labeled “LOD” for limit of detection as discs were 6mm  
958 in diameter.

959

960 **Figure 5: Deployment of an RB-TnSeq library identifies DNA repair mutants**

961 **attenuated for growth on TCBS agar.** (A) Mutant scores for genes known to be  
962 required for *V. cholerae* bile tolerance are shown. In each bar, each datapoint  
963 represents the gene score measured in 1 of 3 biological replicate experiments. A  
964 negative gene score indicates interruption of that gene by transposon insertion had a  
965 deleterious effect, while a positive score indicates a growth advantage. (B) DNA repair  
966 genes meeting quality thresholds (see methods) identified by gene ontology enrichment  
967 using ShinyGO 0.80 are shown. Gene scores are the average of 3 biological replicate  
968 experiments. (C) Serial dilution and spot plating of WT and DNA repair mutant strains  
969 over TCBS agar and LB agar. Plates shown are representative of 3 biological replicates  
970 per strain.

971

972 **Figure 6: RB-TnSeq reveals both component-dependent and independent growth**

973 **defects for *V. cholerae* mutants in TCBS.** (A) Principal component analysis of TCBS  
974 complete and TCBS base (with and without individual selective components, Table 1) by  
975 gene scores. For each condition, individual experimental replicates are plotted in the

976 same color and connected by lines. Plot was generated in R version 4.3.2 using the  
977 package *vegan*. (B) A wide array of mutants are attenuated for growth in TCBS base  
978 supplemented with ox bile. Genes shown in heatmap meet quality thresholds (see  
979 methods). Gene scores are the average of 3 biological replicate experiments. (C) Gene  
980 scores across media demonstrate component-dependent defects for *V. cholerae*  
981 mutants. Each dot in each bar represents the gene's score in one of three biological  
982 replicate experiments. Dashed vertical lines were added to separate genes.

983

984 **Figure S1: *V. cholerae* mutants attenuated for growth in TCBS broth.** (A) All genes  
985 shown meet score thresholds as described in Methods. Gene scores shown are the  
986 average of 3 biological replicate experiments. (B) Genes from S1 that fit into a common  
987 cellular process are grouped by black labels. Gene scores shown are the average of 3  
988 biological replicate experiments.

989

990

**Table 1.) Components of Thiosulfate-Citrate-Bile Salts-Sucrose medium.**

Individual components masses per 1L of TCBS broth. Components thought to be selective are written in bold. pH ~8.6 at 25°C.

Sucrose	20g
Peptone	10g
Yeast extract	5g

Sodium chloride	10g
<b>Sodium citrate</b>	10g
<b>Ox bile</b>	5g
<b>Sodium cholate</b>	3g
<b>Ferric citrate</b>	1g
<b>Sodium thiosulfate</b>	10g

991

Mutants collected	77,678
Mapped barcodes	43,751
Off-by-one barcodes masked	7,361 (16.82%)
Usable, mapped barcodes	36,691 (83.86%)
Unique insertion sites	29,988
Central 80% CDS insertions	23,252
Unique central insertion sites	19,108 (82.18%)
Protein-coding genes in <i>V. cholerae</i>	3,571
With central insertions	2,833 (79.33%)

992

993

994



## Figure 1.) *xseA* mutant *V. cholerae* cannot grow on TCBS agar

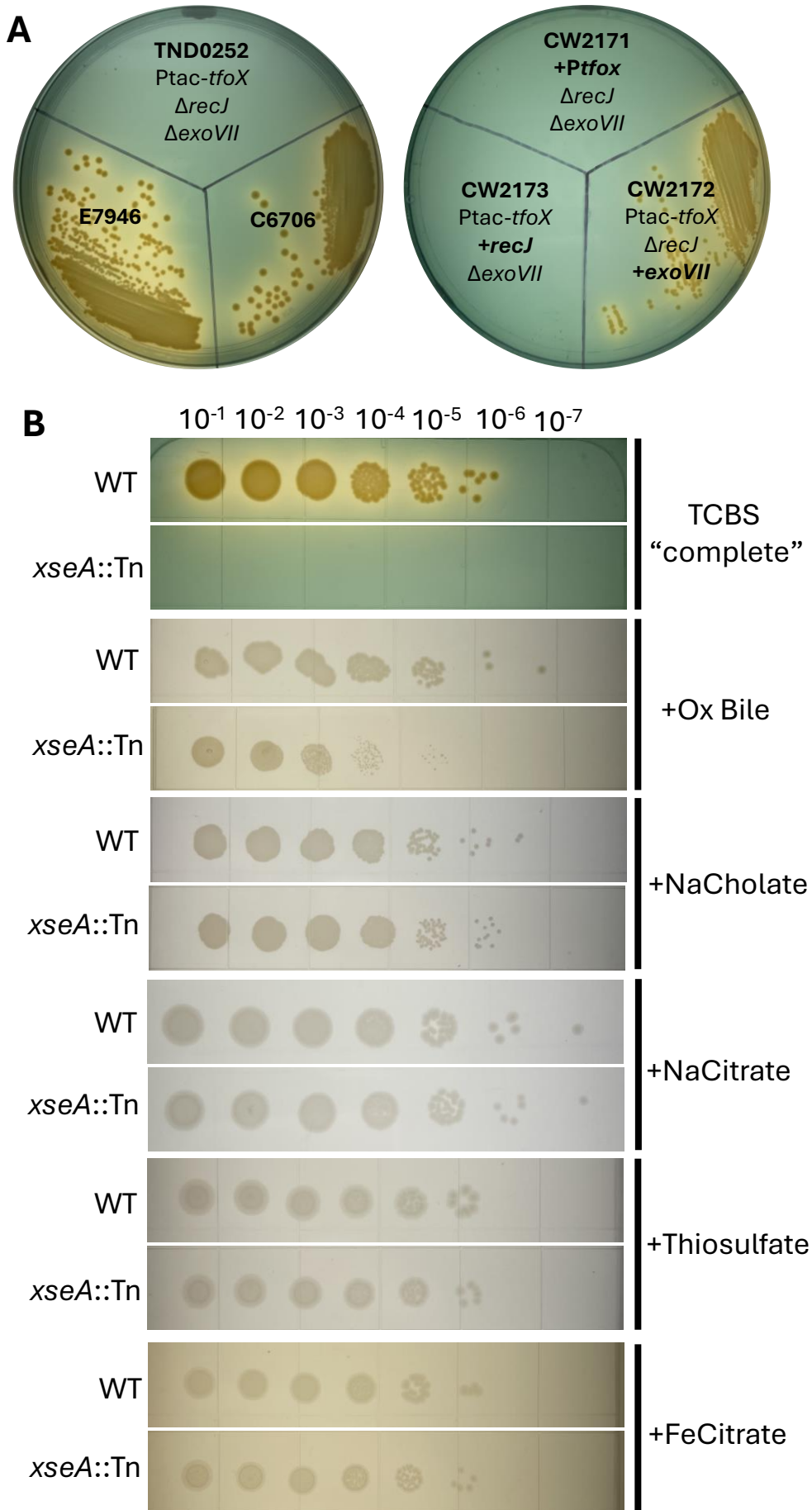






Figure 3.) *exoVII* deficient *V. cholerae* is hypersensitive to ox bile and ciprofloxacin, which can both be suppressed by DNA gyrase mutations.

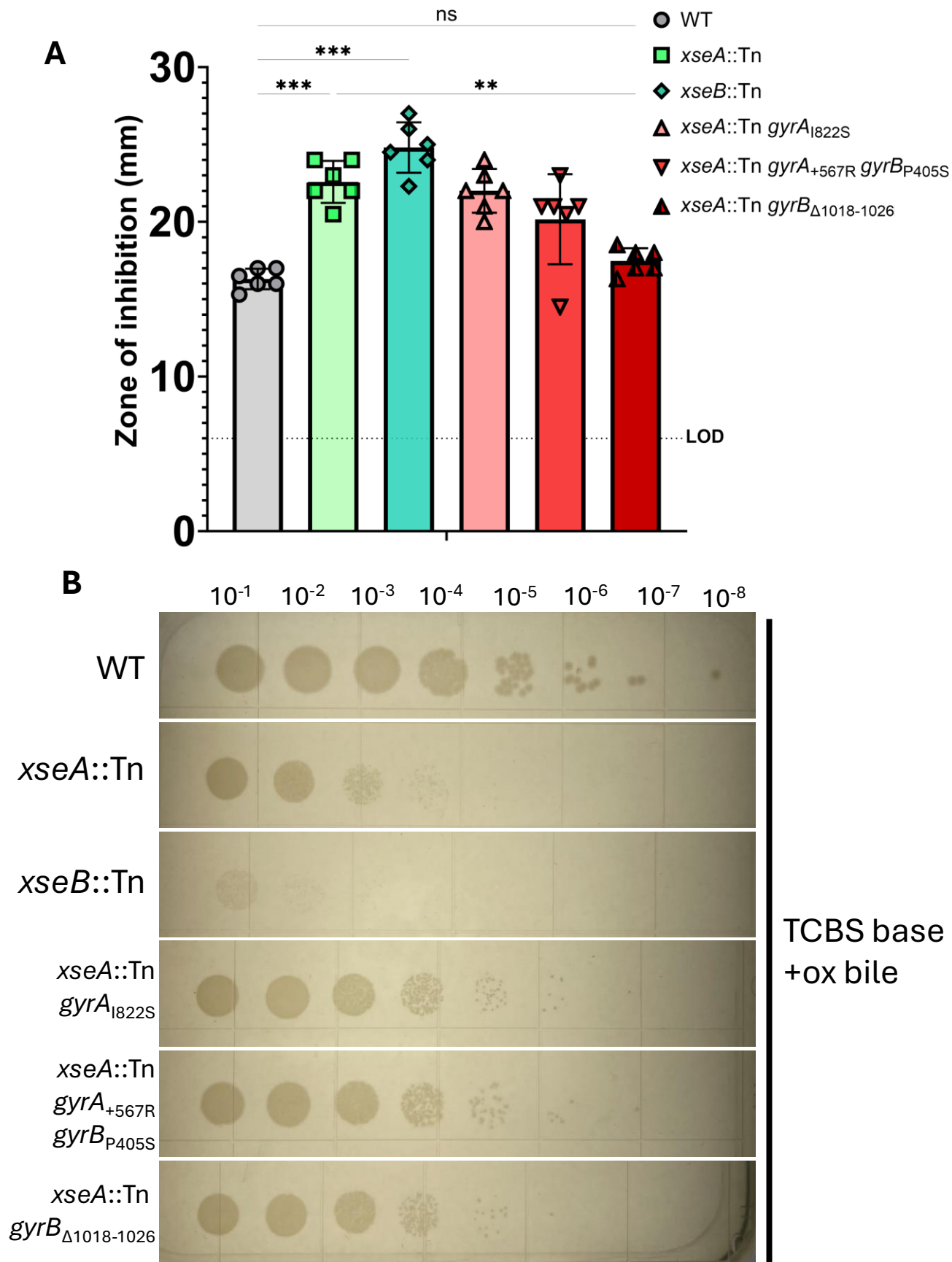
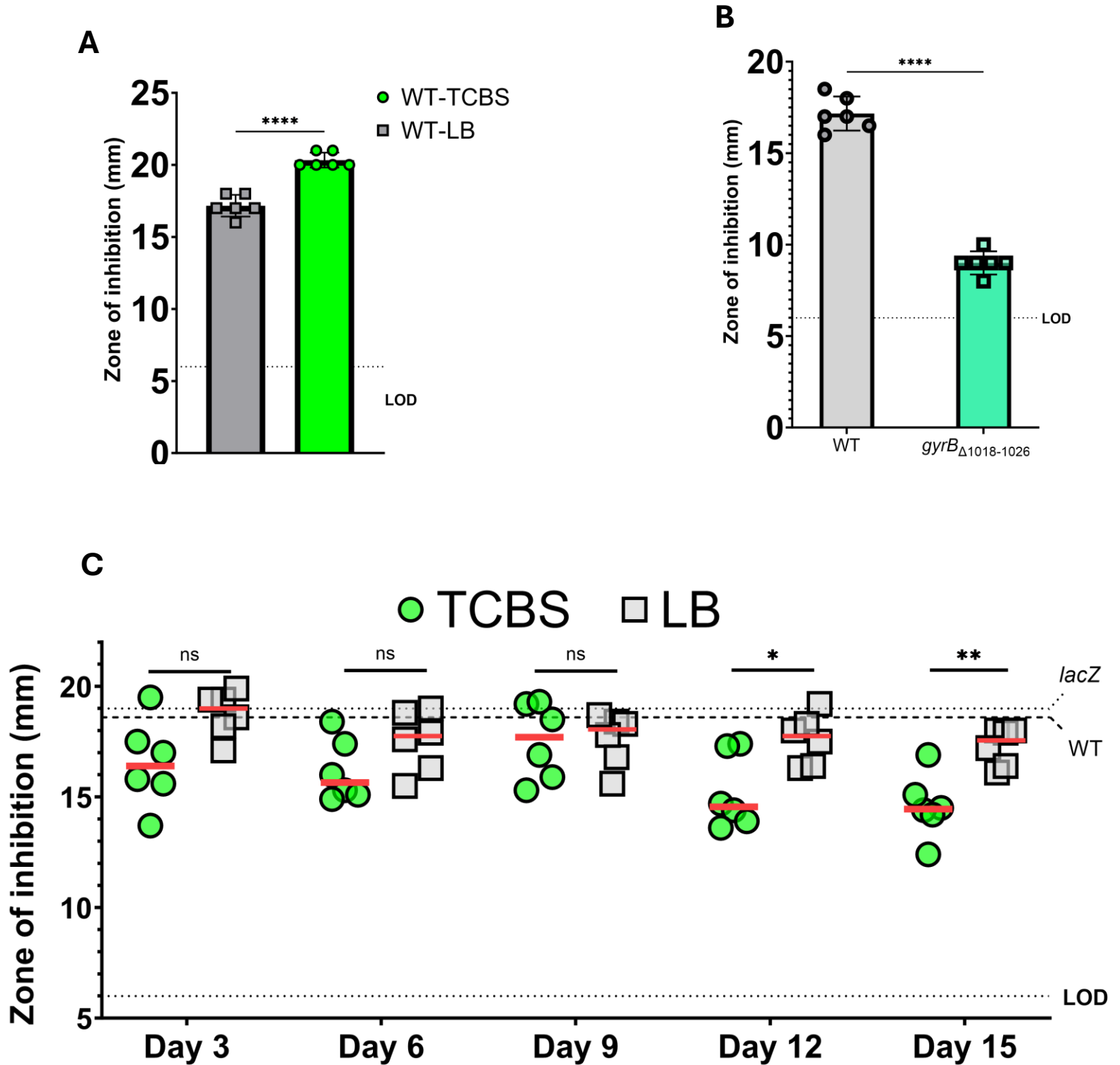
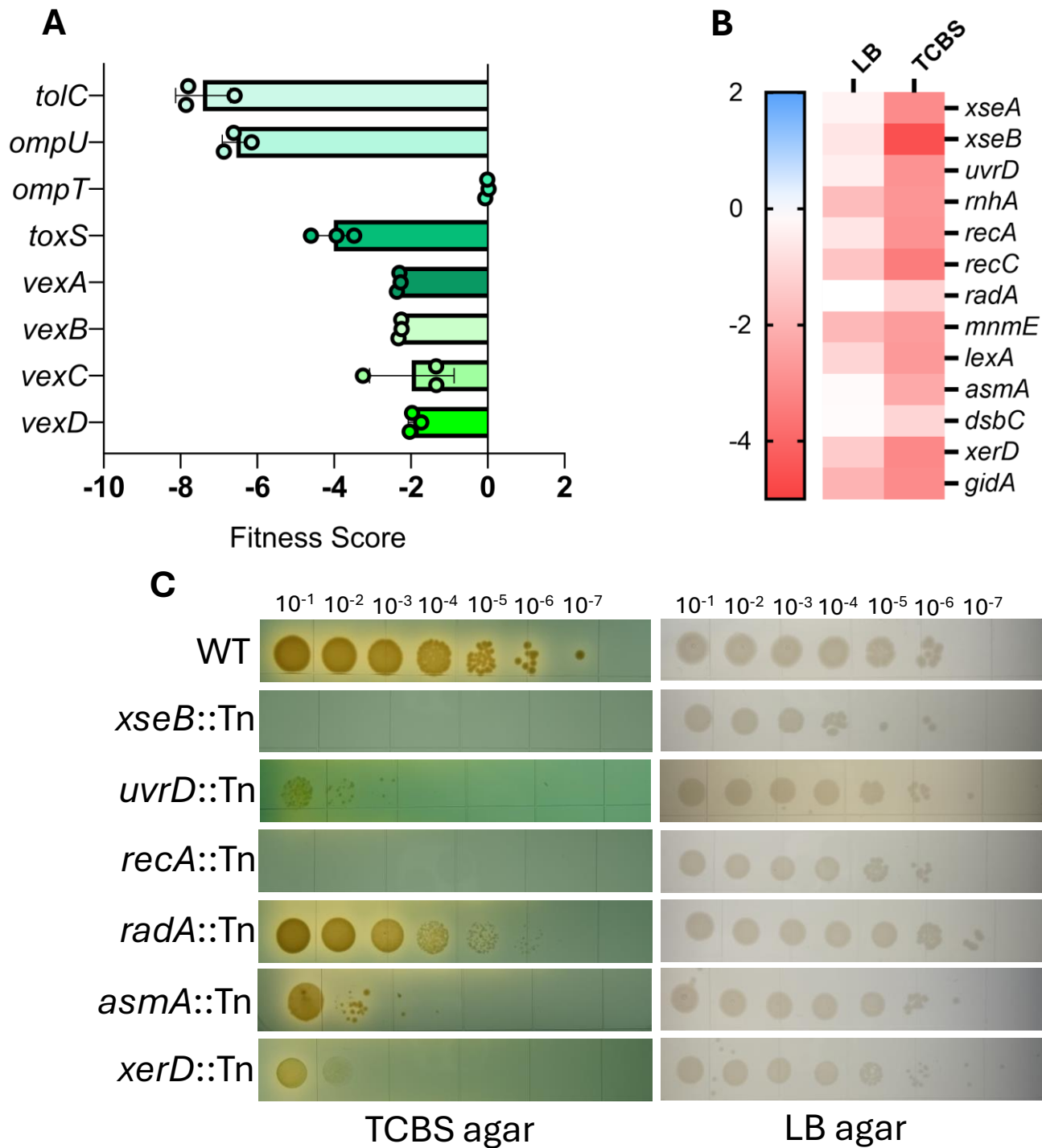


Fig. 4.) Passaging *V. cholerae* on TCBS agar selects for ciprofloxacin resistance



## Figure 5.) Deployment of a randomly-barcoded TnSeq (RB-TnSeq) library identifies DNA repair mutants attenuated for growth in TCBS



# Figure 6.) RB-TnSeq reveals component-wise growth defects for *V. cholerae* mutants in TCBS.

